

## GETTING HOT BY NANOFLARES

David Berghmans

Royal Observatory of Belgium, Ringlaan -3- Avenue Circulaire, B-1180 Brussels, Belgium

### ABSTRACT

We review the current status of the 'Parker hypothesis' which suggests that the solar corona is heated by a multitude of small flare-like events called nanoflares. Space-born coronal imagers such as SXT, EIT or TRACE have allowed to test Parker's hypothesis observationally. Combining the results from different authors it seems that we are close to falsifying the hypothesis, i.e. *there are not enough nanoflares to heat the corona*. The only remaining hope for nanoflare-adepts is the transition region which contains various types of impulsive events such as explosive events or blinkers whose role and mutual relation is not sufficiently understood yet to make a final verdict on Parker's hypothesis.

### 1. FLARE STATISTICS

Flares are the most violent manifestation of solar activity, releasing in only a few minutes huge amounts of energy over the entire electromagnetic spectrum. The most energetic flares, however, are just the tip of the iceberg and progressively more flarelike events are observed for smaller energy releases. During the period 1976-2000, about 50000 flares have been observed by the GOES satellites (Veronig et al. 2002). This comes down to about 1 X-flare per month (0.04/day), an M-flare every 2 days (0.5/day) and several C-flares per day (3.6/day).

The observation that an increasing number of flares is observed at progressively smaller scales, lead Parker (1981, 1983, 1988) to the suggestion that the bulk of the required power to keep the corona at its high temperature might be provided by yet unresolved small flares. Parker introduced the term nanoflare for the hypothetical unobserved flares of about  $10^{24}$  erg of energy release. In fact, a decade earlier Levine (1974) had already proposed a 'new theory of coronal heating' in which he suggested that a multitude of small reconnection events may be responsible for heating of the solar corona.

In recent years we have witnessed the simultaneous operations of superb, space-born coronal imagers

such as SXT (Tsuneta et al. 1991), EIT (Delaboudinière et al. 1995) and TRACE (Handy et al. 1999). These imagers have proven to be specifically useful to study small-scale energy releases for which both an extended FOV -to catch a large number of events- as well as high time resolution is required. Thanks to these imagers, the 'nanoflare' evolved from an hypothetical concept (a flare so small that it is unresolved), to a real world object.

This evolution has allowed to test the Parker's hypothesis observationally. It is well known -see Crosby et al. (1993) for an overview- that the energy distribution  $N(E)$  of the flare energies  $E$  follows a power law

$$N(E)dE = N_0 \left(\frac{E}{E_0}\right)^{-a}. \quad (1)$$

Hudson (1991) noted that if indeed a single power law  $a$  characterizes the whole flare energy distribution, then we can easily evaluate the total heating rate  $W_{tot}$  released by the whole flare family as the integral

$$W_{tot} = \int_{E_{min}}^{E_{max}} N(E)E dE, \quad (2)$$

from the lowest energy ( $E_{min}$ ) flares to the most energetic ( $E_{max}$ ) flares. Indeed, plugging expression (2) into integral (1) yields:

$$W_{tot} = \frac{N_0 E_0^2}{(2-a)} \left[ \left(\frac{E_{max}}{E_0}\right)^{(2-a)} - \left(\frac{E_{min}}{E_0}\right)^{(2-a)} \right] \quad (3)$$

Eq. (3) gives the heating released by the flare events as a function of 4 degrees of freedom that characterize the flare distribution: the lower limit  $E_{min}$ , the upper limit  $E_{max}$ , the power law index  $a$  and  $(N_0, E_0)$  which together form a normalization factor.

Inspired by the summary Fig. 14 in Aschwanden & Parnell (2002), we have taken  $E_{max} = 10^{32}$  erg,  $N_0 = 10^{-49} / s \text{ erg cm}^2$  and  $E_0 = 10^{26}$  erg. The  $(N_0, E_0)$  values are intermediate to reported values by different authors for EUV quiet Sun nanoflares and a reasonable extrapolation for soft and hard X-ray observations in active regions. Adopting these values means that the coronal heating rate by flares  $W_{tot}$  is now given by expression (3) as a function of only 2 free parameters ( $E_{min}$  and  $a$ ) left to determine observationally.

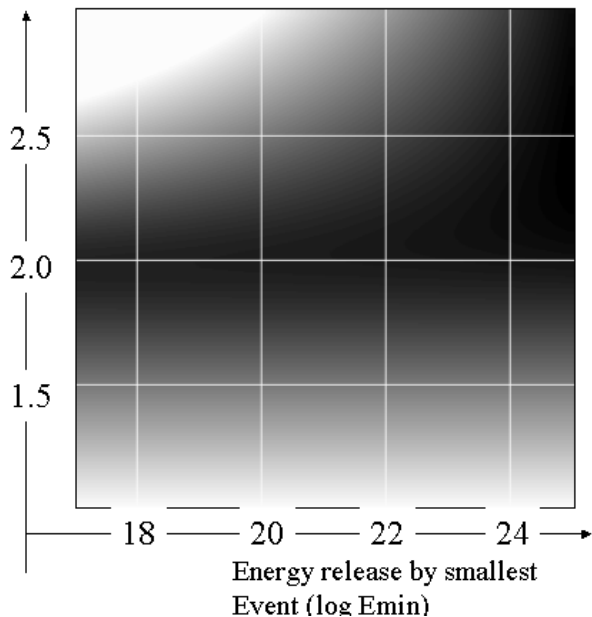
Powerlaw  
index (a)

Figure 1.  $W_{tot}$  as given by Eq. (3) and assuming  $N_0 = 10^{-49}/s \text{ erg cm}^2$ ,  $E_0 = 10^{26} \text{ erg}$  and  $E_{max} = 10^{32} \text{ erg}$ . The brightness scaling is logarithmic.

In Fig. 1 we have plotted  $W_{tot}$  as a function of these 2 free parameters. There are obviously 2 different regimes: if  $a < 2$  (bottom half of Fig. 1) then the total heating is almost independent of the lower limit  $E_{min}$ , since the bulk of the heating is delivered by large events; if  $a > 2$  (top half of the Fig. 1), then the total heating is determined by the lower limit  $E_{min}$  and the bulk of the heating is delivered by small events.

In Fig. 2 we have replotted the same graph but now with the color scale thresholded at the typical heating requirement (Whitbroe & Noyes 1977) for active regions ( $W_{tot} = 10^7 \text{ erg/s cm}^2$ ) and for the quiet Sun ( $W_{tot} = 3 \cdot 10^5 \text{ erg/s cm}^2$ ). Parameter ( $E_{min}, a$ ) combinations in the black area do not lead to sufficient heating of the solar corona. Red areas correspond to parameters ( $E_{min}, a$ ) that do lead to sufficient heating both in the quiet Sun and in active regions. The intermediate, light green bands produce only sufficient heating for the quiet Sun, but not for active regions. It is important to remember that to produce Fig. 1 and Fig. 2, we have assumed  $E_{max} = 10^{32} \text{ erg}$ . Such very energetic flares, however, are only seen in active regions and thus Fig. 1 and Fig. 2 are not valid for the quiet Sun. Replotting Fig. 2 with  $E_{max} = 10^{28} \text{ erg}$  makes the lower regime for  $a < 2$  disappear (see background of Fig. 4). This means that while for heating of active regions  $a$  can in principle be both larger than 2 and smaller than 2, for heating of the quiet sun ' $a > 2$ ' is a necessary condition. It is however important to stress that it is not a sufficient condition (see below)!

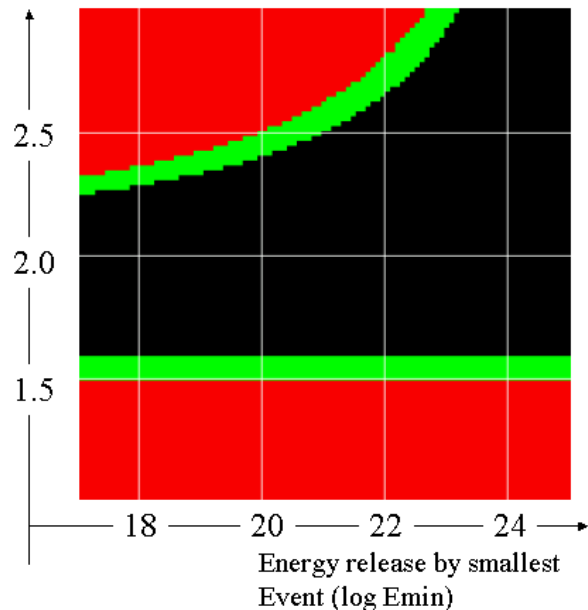
Powerlaw  
index (a)

Figure 2. Same as Fig. 1 but now the color scale has been thresholded at the levels  $W_{tot} = 3 \cdot 10^5 \text{ erg/s cm}^2$  and  $W_{tot} = 10^7 \text{ erg/s cm}^2$  which correspond to the required heating rate of the quiet Sun and of active regions respectively (Whitbroe & Noyes 1977).

## 2. ACTIVE REGIONS

Using data from the Hard X-ray Burst spectrometer (HXRBS) on the Solar Maximum Mission (SMM), Crosby et al. (1993, see also references therein) collected frequency distributions from 12776 solar flares in the periode 1980-1989. They found that all distributions can be represented by power laws above the HXRBS sensitivity threshold. For the distribution of the energy contained in the flare electron flux, a power law of  $a = 1.53 + / - 0.02$  was found in the range  $5 \cdot 10^{28}$  to  $10^{32} \text{ erg}$ . This observed value of the power law is at the edge of the area in Fig. 2 where the heating requirements for active regions are fulfilled.

Crosby et al. (1993) had only access to strong flares because they were looking at full sun integrated (ie non-imaging) hard X-ray fluxes. Using the Hard X-Ray Imaging Spectrometer (HXIS) onboard the Solar Maximum Mission (SMM), Schadee et al. (1983) were the first to describe observations of short-lived X-ray brightenings with hard X-ray fluxes  $10^{-3}$  smaller than regular flares. On the basis of soft X-ray image sequences of the Soft X-ray telescope (SXT, on board Yohkoh), Shimizu and co-workers were able to clearly identify a set of events that they called 'Active region transient brightenings' (ARTBs) (Shimizu et al. (1992,1994) and Shimizu & Tsuneta (1997). These ARTB corresponds to the smallest peaks in the GOES lightcurves, which

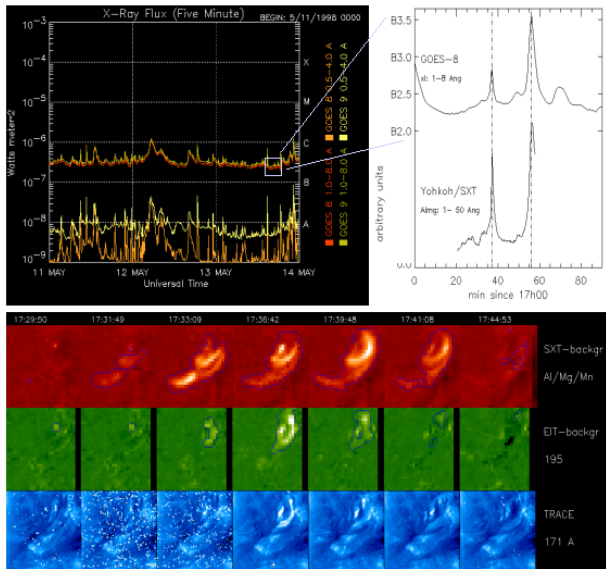


Figure 3. Example showing how the smallest fluctuations in the GOES X-ray lightcurve (top) correspond to small flare-like events -or active region transient brightenings (ARTBs)- clearly seen with imagers such as SXT, EIT and TRACE.

are the reference for flare classifications (see Fig. 3). They take the form of sudden brightenings of magnetic loops and last from a few minutes to tens of minutes. They have a thermal energy content in the range  $10^{25}$  to  $10^{29}$  erg, and their frequency of occurrence (1-40 events per hour per active region) has a strong correlation to the total soft X-ray flux of the active region (Shimizu et al. 1992).

To demonstrate that ARTBs show, just as do ‘regular’ flares, evidence for the acceleration of nonthermal electrons, the soft X-ray observations of ARTB have been combined with simultaneous hard X-ray and radio observations (Gopalswamy et al. 1994, 1997; White et al. 1995; Nindos et al. 1999). The hard X-ray emission of the ARTBs is most noticeable during the rise phase. Just as for regular flares, this hard X-ray emission is most likely explained by precipitating electrons thermalizing in the chromosphere (Nitta 1997). The non-thermal radio emission in the rise phase is presumably due to gyrosynchrotron emission of relativistic electrons (Gary et al. 1997). In ARTBs, the delay of soft X-rays relative to centimeter radio emission and hard X-ray emission is between 1.5 and 6.4 minutes, similar to the well known delay in regular impulsive flares (Neupert 1968). Combining all these results, one arrives to the unavoidably conclusion that ARTBs are indeed most likely scaled down flares, the biggest among them corresponding to the GOES class B flares (see Fig. 3).

When the rate of occurrence of ARTBs is examined as a function of their energy (Shimizu et al. 1994, 1995), the distribution is in the shape of a power law with index  $a = 1.5 - 1.6$ . This range is compatible with the power law of  $a = 1.53$  found for the

distribution of total energy in solar flares (Crosby et al. 1993) and is thus again at edge of the area (Fig. 2) where the heating requirements for active regions are fulfilled. Shimizu (1995) stated for a specific active region in his study, that the total energy released by the sum of the transient brightenings is at most a factor of 5 smaller than the heating rate required. Later results (Berghmans et al. 2001) however indicated that the ARTB detection software used by Shimizu possibly missed a considerable fraction of the events.

Moreover, it is possibly that the number and energy of the ARTBs are underestimated, since only events observed in soft X-rays were taken into account. From earlier space missions like SMM, Skylab or HRTS it was already known that EUV ‘bursts’ or impulsive variations occur nearly continuously in active regions (Withbroe et al. 1985, Habbal et al. (1985)). Simultaneously observations by SXT, EIT, and TRACE (Berghmans et al. 2001), show that the strongest brightenings observed by EIT are indeed the EUV counterparts of the ARTBs seen by SXT. Weaker brightenings seen by EIT often do not have an X-ray counterpart. Among the brightenings detected with SXT a new subpopulation was discovered, consisting of events that brighten in soft X-rays only, at a footpoint of a pre-existing SXT loop shortly after an ARTB occurred at the other footpoint. The propagation speed of the perturbation suggests an interpretation in terms of slow mode MHD waves (Berghmans & Clette 1999, Robbrecht et al. 2001, De Moortel et al. 2002) A scenario is conceivable (Benz & Krucker 2002) where waves travel from the energy release site across and/or along the magnetic field. The superposition of waves from many events could form a quasi-steady turbulent background. Such an energy input amounts to “dark power” as it does not manifest itself in localised intensity brightenings.

### 3. QUIET SUN

In section 1 we pointed out that although the overall heating requirements of the quiet corona are lower than those in active regions, the absence of large flares in the quiet corona means that the heating requirement must be met with small flares only. In the background of Fig. 4 we show the area of parameter ( $E_{min}, a$ ) combinations that do fulfill the heating requirement of the quiet Sun.

Krucker et al. (1997) first reported on soft X-ray brightenings in the quiet Sun with total radiative losses around  $10^{25}$  erg, or more than a magnitude smaller than previously reported X-ray bright points or active region transient brightenings. By comparing the signature of 4 events observed simultaneously in soft X-rays and in radio emission, Krucker & Benz concluded that these events were flare-like and called them network flares. Soon thereafter, Berghmans et al. (1998) reported that wide FOV image sequences in the Fe XII bandpass of the Extreme Ultraviolet

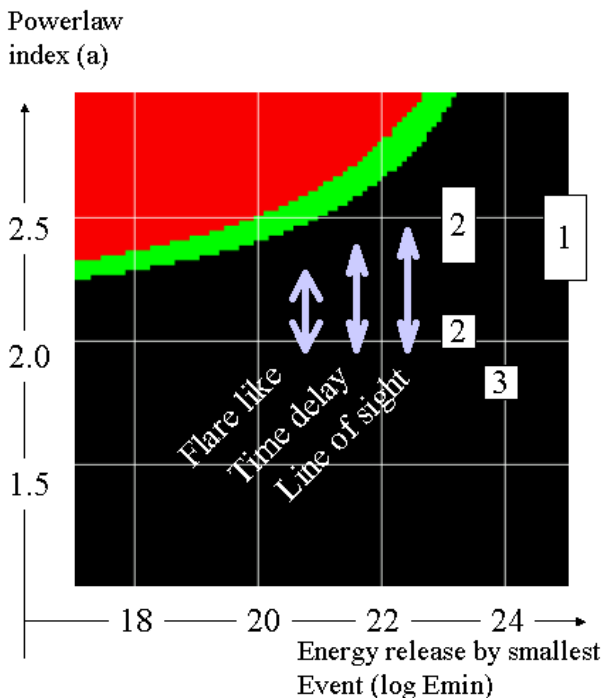


Figure 4. In the background we show  $W_{tot}$  (Eq. 3) under the assumption  $N_0 = 10^{-49}/s \text{ erg cm}^2$ ,  $E_0 = 10^{26} \text{ erg}$  and  $E_{max} = 10^{28} \text{ erg}$  which is appropriate for the quiet Sun. Just as in Fig. 2, the brightness scale has been thresholded at the levels  $W_{tot} = 3 \cdot 10^5 \text{ erg/s cm}^2$  and  $W_{tot} = 10^7 \text{ erg/s cm}^2$  which correspond to the required heating rate of the quiet Sun and of active regions respectively (Whitbroe & Noyes, 1977). The white boxes correspond approximately to the results obtained by (1) Krucker and Benz (1998), (2) Parnell and Jupp (2000) and (3) Aschwanden et al. (2000). The arrows indicate the uncertainty range in the power law index due to the different effects discussed in the text.

Imaging Telescope (EIT) showed hundreds of similar events.

This fact allowed for various large scale statistical studies with EIT (Krucker & Benz 1998) and TRACE (Parnell & Jupp, 2000; Aschwanden et al. 2000). Each of these authors found a power law for the energy distribution of the small scale flares. In Fig. 4 we have plotted the results from the different authors on the position of the power law  $a$  they report and the position  $E_{min}$  corresponding to the lower limit of their power law.

Although none of the reported results falls into the green or red area, this in itself does not falsify Parker's hypothesis. The lower end of the power law is typically limited by the sensitivity and resolution of the instruments and method used. One can assume that e.g. if the power law  $a = 2.3-2.6$  reported by Krucker & Benz (1998, box '1' in Fig. 4) extends further downward beyond the instrument resolution and sensitivity, down to e.g.  $E_{min} = 20 \text{ erg}$ , the quiet corona would indeed be sufficiently heated. At

the other hand, the much flatter power law reported by Aschwanden et al. (2000),  $a = 1.8$ , would never lead to sufficient heating, no matter how far the validity of the power law would extend beyond the observed  $E_{min}$ . This essential difference between the results from different authors is discussed in the next section.

#### 4. REASONS FOR DISCREPANCIES

The discrepancies between the results of different authors in Fig. 4 are striking. It is important to realize that these differences are not 'random' nor 'data noise' but that they are the effect of choices in the way the data is interpreted. To clarify this, we will quickly overview in this paragraph the main steps in the analysis of a dataset for nanoflare statistics. There are essentially 3 main steps: (1) detection: look for very small flares, (2) evaluation: determine how much each of them contributes to the coronal heating, (3) statistics: count them.

When on the hunt for nanoflares, a first is choosing a dataset. This means a choice of wavelength or bandpass (e.g. soft X-rays or a EUV channel), but also the choice of a spatial and temporal resolution. When choosing a bandpass corresponding to a lower temperature regime in the corona, one will sample more 'weak' events than when using a 'hot' bandpass. When the temporal resolution is high, one can sample more short-lived events than with a lower temporal resolution. It is thus no surprise to find different result for different datasets.

Once a dataset has been chosen, one needs to identify nanoflares by selecting pixel values that exceed a certain brightness threshold. The choice of the level of this brightness threshold again influences the power laws. Krucker & Benz (1998) show that when a less restrictive (lower) threshold is used ( $3 \sigma$  instead of  $5 \sigma$ ), more 'weaker' events are selected and the power law can decrease from 2.59 to 2.31!

When the pixels showing brightenings have been detected, they must be grouped in events. It is obvious that 2 neighboring pixels brightening at exactly the same time correspond to the same event and must be grouped. When the brightening pixels are not immediate neighbors and/or when their brightening is not exactly simultaneously, again a choice must be made. Benz & Krucker (2002) showed that relaxing simultaneity from 1 to 3 min leads to a change in the power law of 0.33. Also in the spatial dimensions, being tolerant when merging pixels in events leads to big events some of which are artificially merged independent events. Being restrictive leads to small events some of which are artificial splits of events that belong together.

Aschwanden et al. (2000) have argued that it is necessary to impose an extra criteria to distinguish the flare-like events (increase in temperature in a loop like area) from the many other phenomena that

might lead to localised intensity enhancement (eg waves, motions of large loops, moss, bad data,...). Selecting only flare-like events can lower the power law by 0.3 (Aschwanden et al. 2000) because there is a higher chance among the weak/small events to be non-flaring than among the strong/large events.

Once the events have been identified, we need to evaluate how much each of the detected events contributes to the coronal heating. Calculating the energy release of the events requires another set of choices/assumptions. The usual approach is to calculate the thermal energy  $E_{th}$  of the events with the formula

$$E_{th} = 3n_e k_B T_{flare} V \quad (4)$$

where  $n_e$  is the electron density,  $T_{flare}$  the peak temperature of the flare and  $V$  the volume of the flaring loop. This last parameter is estimated from the measured flaring area  $A$  and an assumed line-of-sight depth. The choice for a line-of-sight depth has a direct implication on the resulting power law of the energy distribution. Parnell & Jupp (2000) showed that if a constant line-of-sight was assumed, a power law around 2.5 was found, while if a line-of-sight proportional to the square root of the measured flaring area  $A$  was assumed, a power law of the order of 2.0 was found (these two values correspond to the two boxes labeled '2' in Fig. 4. Also fractal dependence have been used to estimate the unobservable line-of-sight (Aschwanden & Parnell 2002). Besides this line-of-sight unknown, various other implicit assumptions and effect can influence the energy estimation of the events. These include plasma expansion, losses during rise time, filling factor and energy losses via motions and waves.

In a third step, the energy distribution of all the events needs to be evaluated as a whole to determine the power law towards progressively smaller events. Various choices needs to be taken in the process (*e.g.* binsize of the histogram, roll-over point,...) that can ultimately influence the error-bars on the power law. In Fig. 4 we have shown arrows that indicate the size of some of the uncertainties discussed above. It is clear from this Fig. that the scatter in results from different authors can indeed be explained by differences in methods.

## 5. REMAINING PROBLEMS

If the previous section would have been the last one, then the overall conclusion would simply be that the observed power law is of the order of perhaps  $a \sim 2.25$  and that the quiet Sun corona could indeed be heated by nanoflares if the flare energy distribution extends down to something like  $E_{min} \sim 10^{18}$  erg. Unfortunately there are two more remaining problems: (1) we probably cannot extrapolate down to whatever  $E_{min}$  is convenient, and (2) all the reported power laws are overestimated due to a systematic bias from the use of narrow band EUV imagers.

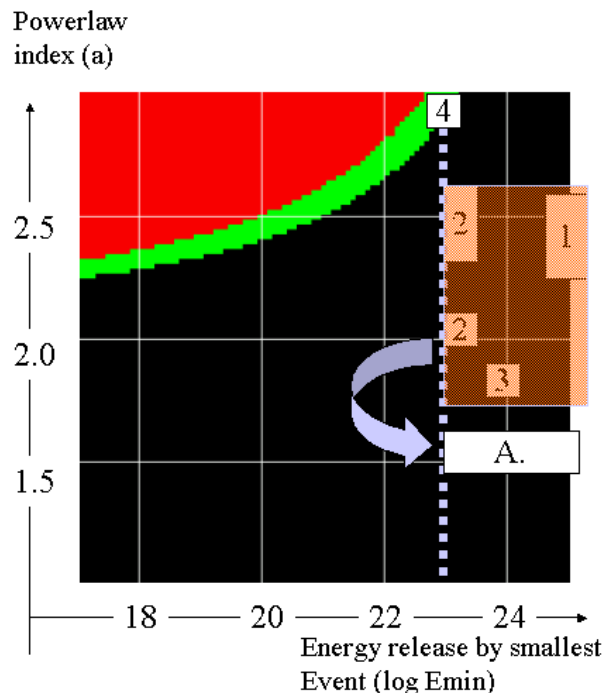


Figure 5. On the same background as in Fig. 4, we have overplotted a vertical dashed line representing the fuzzy lower limit below which no events are expected. The arrow represents the correction for the bias induced by narrowband EUV imagers. The white box numbered 4 correspond to the results by Winebarger et al. (2002).

### 5.1. Limits to extrapolation

By combining observations of EUV nanoflares, SXR transient brightenings, and SXR+HXR flares, Ashwanden (1999) established scaling laws for spatial scales and electron densities, *i.e.*  $L(T) \sim T$  for the footpoint separation  $L$  of flare loops, and  $n_e(T) \sim T^2$  for the average loop density. Based on these two observational findings, Ashwanden derived scaling laws for the loop pressure,  $p(T) \sim T^3$  and the thermal energy  $E_{th} \sim T^6$ .

The temperature dependence of these scalings laws suggests that the smallest flares will be found at relatively low temperatures  $T$ . At the other hand, if we want nanoflares to heat the corona, they cannot be cooler than say  $T = 10^6$  MK. This indicates that physical limits exists that cut-off the distribution of flares at the lower end: we cannot assume whatever  $E_{min}$  that is convenient.

One of these physical limits is the pressure balance between the heated plasma in coronal flare loops and the underlying ambient chromospheric plasma. If the temperature in a flaring loop is too low, the  $p(T) \sim T^3$  will be smaller than the chromospheric pressure and thus the *coronal*, flaring loop simply cannot exist. This chromospheric pressure balance implies a

cutoff in the distribution of flare loop sizes and flare energies. Aschwanden (1999) infers a cutoff in the distribution of flare energies of  $E_{th} \sim 10^{23} - 10^{24}$  erg. We have plotted this cutoff at  $E_{th} \sim 10^{23}$  erg as a vertical dashed line through Fig. 5.

## 5.2. EUV imagers bias

Aschwanden & Charbonneau (2002) pointed out that the use of narrow bandpass EUV imagers such as EIT and TRACE leads to a bias in the calculation of the energy of nanoflares. From the physics of large flares, it is well known that the flare plasma is heated to a maximum temperature and then cools down gradually. The observed intensity through a narrow bandpass imager peaks when the flare plasma has cooled sufficiently down to match the peak response temperature of the narrow bandpass.

This means that when calculating the energy using Eq. (4) one fills in the peak response temperature of the filter  $T_{filter}$  rather than the temperature  $T_{flare}$  of the flaring plasma at peak intensity. Since this underestimation of the flare energy is largest for strong flares (because the energy of the flare is correlated with  $T_{flare}$ ), it means that the narrow bandpass EUV imagers introduce a bias towards artificially steep power laws. Correcting for this effect, (Aschwanden & Parnell, 2002) found that all previously reported power laws in the range  $a \sim 2.0 - 2.3$  fall back to a range  $a \sim 1.5 - 1.6$  (see region 'A' in Fig. 5), which is consistent with results obtained with the broadband imager SXT.

## 6. TRANSITION REGION ?

From Fig. (5) it seems that there is no hope remaining for heating the quiet sun with small-scale flare activity. The extrapolation to small unresolved flares has physical limits and the power law -after correcting for the EUV imagers bias- is too low, even if we would break that limit. Having reached this point, one can argue that the Parker hypothesis has been falsified conclusively. Let us, for the sake of the argument, see if there is any hope to avoid this conclusion.

Since  $E_{th} \sim T^6$ , the smallest flares will liberate their energy at relatively small temperatures. This means that the smallest energy releases are to be expected near the transition region. It may be noted (Benz & Krucker 2002) that the variability increases towards lower temperatures (Berghmans et al. 1998) and has a maximum in the transition region, where the time scales are shorter and the temporal power spectrum the flattest (Benz & Krucker 1999). The cutoff at  $E_{th} \sim 10^{23}$  erg is based on the validity of the derived scaling laws for all flare-like heating events. However, since the physical environment changes drastically at the interface between the corona and the chromosphere, it is indeed not impossible that the

scaling laws derived from coronal events cease to be valid.

Moreover, the transition region harbors various kinds of impulsive events that are not completely understood such as blinkers (Harrison 1997, 1999; Berghmans et al. 1998; Brkovic, Solanki, Ruedi 2001; Bewsher, Parnell and Harrison 2002) as well as explosive events (Brueckner & Bartoe 1983; Dere et al. 1989). Dere et al. (1991) and Dere (1994) suggested that explosive events are small-scale reconnection events. Innes et al. (1997) reported finding a spatial separation between blueshifted and redshifted streams in explosive events, supporting the prediction of Dere et al. Chae et al. (2000) studied in detail the relation between explosive events and blinkers. They found that explosive events tend to occur around blinkers, rather than co-spatial, and that blinkers instead consist of many small-scale, short-lived SUMER "unit brightening events".

In a recent paper, Winebarger et al. (2002), estimated the power law index of the energy distribution of explosive events. Since they select events by their Doppler shift as recorded by SUMER, the detection can be much more sensitive than when looking for intensity variations above a background. Moreover, they do not suffer from the above described narrow-band EUV imager bias. Their result ( $a = 2.9 \pm 0.1$  for the energy range  $10^{22.7}$  erg -  $10^{25.1}$  erg) is indicated in Fig. 5 with label '4', close to or in the area where sufficient heating is released to heat the quiet Sun! However, Winebarger et al. (2002) assumed that each SUMER pixel showing an explosive event is an independent event, i.e. they did not assemble neighboring pixels into events. This might artificially create many small events and thus artificially steepens the power law index. The results by Winebarger et al. (2002) nevertheless show that it is too soon to declare the end of Parker's hypothesis.

## 7. CONCLUSIONS

We reviewed the current status of the 'Parker hypothesis' which suggest that the solar corona is heated by a multitude of small flare-like events called nanoflares. In recent years we have witnessed the simultaneous operations of superb, space-born coronal imagers such as SXT, EIT or TRACE. These imagers have proven to be specifically useful to study small-scale energy release events for which both an extended FOV as well as high time resolution is required. Thanks to these imagers, the 'nanoflare' evolved from an hypothetical concept (a flare so small that is unresolved), to a specific, real world object. This evolution has allowed to test the 'Parker hypothesis' observationally.

Assuming 1 power law dependence for the whole flare family and using the formulas (1)-(3) introduced by Hudson (1991), we focused on 2 free parameters that determine whether nanoflares can provide sufficient

energy to heat the corona or not. These free parameters are the energy  $E_{min}$  released by the smallest flare-like events and the power law index  $a$  that defines how many 'small' events exist relative to the 'large' events.

It is often said that for flaring activity to heat the corona,  $a$  needs to be larger than 2. This statement however oversimplifies the situation. In the quiet Sun,  $a > 2$  is a necessary condition *but not a sufficient* condition. In active regions, even when  $a < 2$  the heating contribution from larger flare like events (*e.g.* ARTB) can contribute a considerable part of the heating.

For both active regions and for the quiet Sun, we have reviewed a selection of observational results. In active regions, a single power law of about 1.5-1.6 seems to represent well the energy distribution from the large flares (Crosby et al. 1993) down to ARTBs (Shimizu et al. 1992). This is on the edge of the area in parameter space (Fig. 2) where flares do contribute sufficient heating to maintain the active regions. It is worth pointing out also, that part of the energy released by flares might be 'dark power', as it remains unobserved in the form of MHD waves propagating throughout the whole corona.

Whereas in the active regions significant coronal heating by flares is possible, the situation is very different for the quiet Sun. As larger flares ( $> 10^{28}$  erg) are absent in the quiet Sun, the heating must be delivered at the lower end of the flare distribution. This puts severe constraints on the parameters  $E_{min}$  ( $< 10^{24}$  erg) and  $a$  ( $> 2.2$ ). Several authors have used data from imagers like SXT, EIT and TRACE to observationally determine the parameters  $E_{min}$  and  $a$ . Their results vary significantly (see Fig. 3). We have explained these differences as being due to methodical uncertainties.

It we take into account that physical limits exist on how small the least energetic flare can be ( $E_{min} \sim 10^{23}$  erg ?) and that most previously reported power laws are too steep due to a methodical bias, it seems that Parker's hypothesis is unfeasible. *Current observations do not show enough nanoflares.*

The only remaining hope for nanoflare-adepts is the transition region which contains various types of impulsive events such as explosive events or blinkers whose role and mutual relation is not sufficiently understood yet to come to a conclusive verdict on Parker's hypothesis. This last hide-out for the nanoflares or -perhaps picoflares- will be checked by the battery of imagers (Atmospheric Imaging Array, AIA) planned for the NASA SDO mission. AIA will image the chromosphere to low corona at a 10 sec cadence, simultaneously in 7 channels, at a TRACE like spatial resolution.

## REFERENCES

- Aschwanden, M.J., 1999, Sol. Phys., 190, 233
- Aschwanden, M.J., Nightingale, R.W., Tarbell, T.D., Wolfson, C.J., 2000, ApJ, 535, 1027
- Aschwanden, M.J., Tarbell, T.D., Nightingale, R.W., Schrijver, C.J., Title, A., Kankelborg, C.C., Martens, P. and Warren, H.P., 2000, ApJ, 535, 1047
- Aschwanden, M.J., Charbonneau, P., 2002, ApJ, 566, L59
- Aschwanden, M.J., Parnell, C.E., 2002, ApJ, 572, 1048
- Berghmans, D. and Clette, F., 1999, Sol. Phys., 186, 207
- Berghmans, D., Mckenzie, D. and Clette, F., 2001, AA, 370 591
- Berghmans, D., Clette, F. and Moses, D., 1998, AA., 336, 1039
- Benz, A.O., Krucker, S., Acton, L.W., Bastian, T.S., 1997, A&A, 320, 993
- Benz, A.O., Krucker, S., 1999, AA, 352, 1083
- Benz, A.O., Krucker, S., 2002, ApJ, 568, 413
- Bewsher, D., Parnell, C.E. and Harrison, R.A., 2002, Sol. Phys, 2002, 21
- Brueckner, G.E., Bartoe, J.-D.F., 1983, ApJ, 272,329
- Brkovic, A., Solanki, S.K. and Ruedi, I., 2001, AA, 373, 1056
- Chae, J., Wang, H. and Goode, P.R., 2000, ApJ, 528, L119
- Crosby, N.B., Aschwanden, M.J. and Dennis B.R., 1993, Sol. Phys., 143, 275
- Delaboudinière, J.-P. et al. 1995, Solar Phys., 162, 291
- Dere, K.P., Bartoe, J.-D.F., Brueckner, G.E., 1989, Sol. Phys., 123, 41
- Dere, K.P., Bartoe, J.-D.F., Brueckner, G.E., Ewing, J. & Lund, P. 1991, JGR, 96, 9399
- Dere, K.P., 1994, Adv. Space Res., 14, 13
- De Moortel, I., Ireland, J., Walsh, R.W., Hood, A.W., 2002, Sol. Phys., 209, 61
- Gary, D.E., Hartl, M.D., Shimizu, T., 1997, ApJ, 958
- Gopalswamy, N., Payne, T.E.W.,Schmahl,E.J., Kundu, M.R., Lemen, J.R., Strong, K.T., Canfield, R.C. and J. De La Beaujardiere, 1994, ApJ, 437, 522
- Gopalswamy, N., Zhang, J., Kundu, M.R., Schmahl, E.J. and J.R. Lemen, 1997, ApJ, 491, L115
- Habbal, S.R., Ronan, R. and Withbroe, G.L. , 1985, Solar Phys., 98, 223
- Handy, B.N., et al., 1999, Sol. Phys. 187, 229
- Harrison, R.A., 1997b, Sol. Phys., 175 (part 2), 467
- Harrison, R.A., Lang, J., Brooks, D.H. and Innes, D.E., 1999, AA, 351, 1115
- Hudson, H.S. 1991, Solar Phys., 133, 357
- Innes, D.E., Inhester, B., Axford, W.I., Whilhelm, K., 1997, Nat, 386, 24, 811

- Krucker, S., Benz, A.O., Bastian, T.S. and Acton, L.W., 1997, ApJ, 488, 499
- Krucker, S., Benz, A.O., 1998, ApJ, 501, L213
- Levine, R.H., 1974, ApJ, 190, 447
- Neupert, W.M., 1968, ApJ, 153, L59
- Nindos, A., Kundu, M.R., White, S.M., 1999, ApJ, 513, 983
- Nitta, N., 1997, ApJ, 491, 402
- Ogawara, Y., Takano, T., Kato, T., Kosugi, T., Tsuneta, S., Watanabe, T., Kondo, I., Uchida, Y., 1991, Sol. Phys., 136, 1
- Parker, E.N., 1981, ApJ, 244, 644
- Parker, E.N., 1983, ApJ, 264, 642
- Parker, E.N., 1988, ApJ, 330, 474
- Parnell, C.E. and Jupp, P.E., 2000, ApJ, 529, 554
- Robbrecht, E., Verwichte, E., Berghmans, D., Hochedez, J.F., Nakariakov, V.M. and Poedts, S., 2001, A&A, 370, 591
- Schadee, A., de Jager, C. , Svestka, Z., 1983, Sol. Phys., 89, 287
- Shimizu, T., Tsuneta, S., Acton, L.W., Lemen, J.R. and Uchida, Y., 1992, PASJ, 44, L147
- Shimizu, T., Tsuneta, S., Acton, L.W., Lemen, J.R. , Ogawara, Y. and Uchida, Y., 1994 ApJ, 422, 906
- Shimizu, T., 1995, PASJ, 47, 251
- Shimizu, T., Tsuneta, S., 1997, Astrophys. J., 486,1045
- Tsuneta, S., Acton, L., Bruner, M., Lemen, J., Brown, W., Carvalho, R., Catura, R., Freeland, S., Jurcevich, B., Owens, J., 1991, Sol. Phys., 136, 37
- Veronig, A., Temmer, M., Hanslmeier, A., Otruba, W., Messerotti, M., 2002, AA, 382, 1070
- White, S.M., Kundu, M.R., Shimizu, T., Shibasaki, K., Enome, S., 1995, ApJ, 440, 435
- Withbroe, G.L., Habbal, S.R. and Ronan R., 1985, Solar Phys., 95, 297
- Withbroe, G.L. and Noyes, R.W., 1977, ARA&A, 15, 363
- Winebarger, A. R., Gordon Emslie, A., Mariska, J.T., Warren, H.P., 2002a, ApJ, 565, 1298